ChemComm

Accepted Manuscript

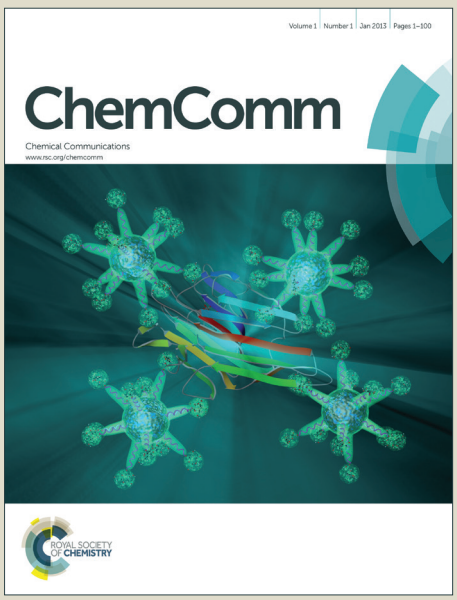

ROYAL SOCIETY OF CHEMISTRY

www.rsc.org/chemcomm

Cite this: DOI: 10.1039/c0xx00000x

www.rsc.org/xxxxxx

ARTICLE TYPE

Mesoporous "Shell-in-Shell" Structured Nanocatalyst with Large Surface Area, Enhanced Synergy, and Improved Catalytic Performance for Suzuki-Miyaura Coupling Reaction

Baocang Liu,[a,b,c] Yuefang Niu,[a] Yan Li,[a] Fan Yang,[a] Jiamin Guo,[a] Qin Wang,[a,c] Peng Jing,[a] Jun Zhang,*[a,b,c], and Guohong Yun[c]

Received (in XXX, XXX) Xth XXXXXXXXX 20XX, Accepted Xth XXXXXXXXX 20XX

DOI: 10.1039/b000000x

A novel mesoporous "shell-in-shell" structured nanocatalyst (@Pd/meso-TiO_2/Pd@meso-SiO_2) with large surface area, enhanced synergy, and improved catalytic performance is created for catalyzing Suzuki-Miyaura coupling and 4-nitrophenol reduction reactions.

Heterogeneous catalysis, as a promise route to obtain desired targets, has aroused great research interests because it is widely applicable in various catalytic reactions with good recovery capacity and recyclability.[1] Noble metal nanocatalysts have been widely investigated in heterogeneous catalysis.[2,3] However, the noble metal nanocatalysts tend to aggregate, leading to the loss of catalytic activity under high temperature treatment or reaction condition.[4] Loading noble metal nanoparticles on surface-modified supports is an ideal approach to solve this problem,[5,6] because the diverse supports can limit the migration of noble metal nanoparticles and prevent against aggregation. In addition, the synergetic effects between the noble metal nanoparticles and the supports are in favor of improving catalytic performance.[7]

Among the investigated metal oxide supports, TiO_2 is the most promising one due to its excellent redox ability and chemical and thermal stability.[8] In order to pursue the optimum catalytic performance, TiO_2 with diverse morphologies have been widely studied.[9,10] Among these studies, hollow mesoporous TiO_2 nanocatalyst is the mostly involved one in recent years, due to its superior catalytic property.[11-13] Furthermore, the TiO_2 nanocatalyst can be futher integarted by loading the noble metal nanoparticles in the cavity,[14,15] on the internal[16] or external surfaces of hollow TiO_2 sphere[17] to enhance its catalytic performance.

Mesoporous SiO_2 (meso-SiO_2) coating is an effective route to improve the stability of nanocatalysts.[18,19] The meso-SiO_2 shell can resist the aggregation of active species, reduce the leaching of noble metal, and improve the accessibility of active species.[20] Meanwhile, the selectivity for reactants also can be tuned via changing the pore size of meso-SiO_2 and hydrophilic or hydrophobic of meso-SiO_2 surface.[21,22] Furthermore, resorcinol-formaldehyde (RF)-resin polymerization, as a common easily removeable hard template, has been widely to synthesize carbon spheres[23] and various hollow sphere materials.[24, 25]

Herein, we design a novel mesoporous "shell-in-shell" structured nanocatalyst (@Pd/meso-TiO_2/Pd@meso-SiO_2). The nanocatalyst is composed of mesoporous double TiO_2 and SiO_2 shells with the ultrafine Pd nanoparticles (PNPs) uniformly distributed on the external and internal surfaces of meso-TiO_2 shell. Such structrual configuration endows the nanocatalyst large surface area due to the mesoporous shells, enhanced synergy between PNPs and TiO_2 shell, independent chambers formed by two shells. Untimately, the nanocatalyst, which is explored used as an effective nanoreactor, exhibits improved catalytic activity and selectivity for Suzuki-Miyaura coupling reaction and highly catalytic activity and stability for 4-nitrophenol reduction reaction. Depending on the restriction of mesopores of the outer meso-SiO_2 shell on reactant molecules, the catalytic selectivity for Suzuki-Miyaura coupling is sucessfully realized.

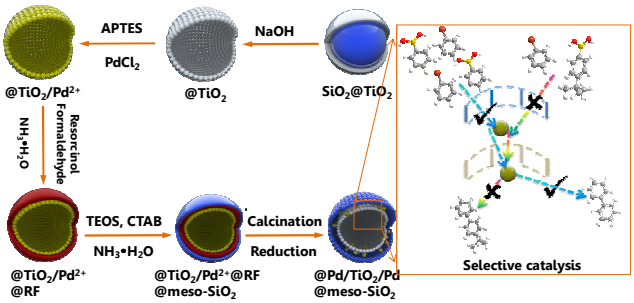

Scheme 1. Schematic illustration showing the synthsis of "shell-in-shell" @Pd/meso-TiO_2/Pd@meso-SiO_2 nanocatalyst.

The synthesis of "shell-in-shell" structured @Pd/meso-TiO_2/Pd@meso-SiO_2 nanocatalyst follows the procedures illustrated in Scheme 1. Initially, a layer of TiO_2 is coated onto SiO_2 spheres via a sol-gel process to obtain SiO_2@TiO_2 spheres. Then, the SiO_2 spheres are removed by etching with NaOH solution to obtain @TiO_2 spheres. After modifying the @TiO_2 spheres with -NH_2 groups using 3-aminopropyl)triethoxysilane (APTES) to render a hydrophilic surface, Pd^{2+} ion-diffusion process is carried out. With this step, Pd^{2+} ions can be diffused easily into the central cavity of the @TiO_2 spheres through mesoporous TiO_2 shells. Then, the @TiO_2 spheres with Pd^{2+} ions loaded on the internal and external surfaces are subsequently coated with the layers of resorcinol formaldhyde (RF)

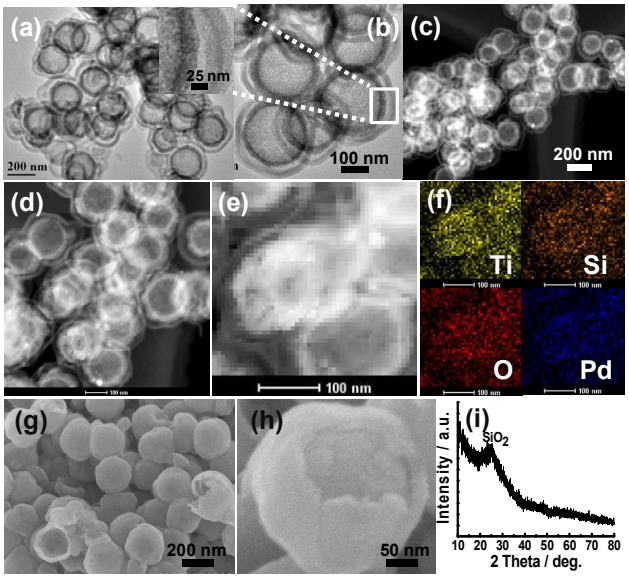

Fig. 1 TEM (a and b), STEM (c, d, and e), SEM images (g and h), and XRD pattern (i) of "shell-in-shell" @Pd/meso-TiO_2/Pd@meso-SiO_2 nanocatalyst; (f) EDX elemental mapping of Ti, Si, O, and Pd in "shell-in-shell" @Pd/meso-TiO_2/Pd@meso-SiO_2 nanocatalyst shown in (e). The inset image of (a) is the partically enlarged image of (b) showing the existence of meso-porosity in TiO_2 and SiO_2 shells.

and mesoporous SiO_2. Following the calcination and reduction under hydrogen atmosphere, the @Pd/meso-TiO_2/Pd@meso-SiO_2 nanocatalyst is obtained.

The resulting @Pd/meso-TiO_2/Pd@meso-SiO_2 nanocatalyst shows good monodispersibility and possesses well-defined "shell-in-shell" structrual configuration consisting of mesoporous TiO_2 and SiO_2 shells with ultrafine PNPs loaded on both internal and external surfaces of meso-TiO_2 shell (Figs. 1a, b, S3, and S4). The diameters of hollow TiO_2 and SiO_2 spheres are estimated to be ~170 and ~300 nm, respectively. The thickness of TiO_2 and SiO_2 shells are around ~35 and ~24 nm, respectively. The mesopores on TiO_2 and SiO_2 shells can be clearly observed from the enlarged image (Inset in Fig. 1a). Due to the "shell-in-shell" structural feature, a interlayer chamber of ~50 nm is created. The STEM images further confirm the "shell-in-shell" structural configuration with a interlayer chamber exsiting between TiO_2 and SiO_2 shells (Fig. 1c, d, and e). In addition, light spots on both sides of TiO_2 shells further suggest the good distribution of PNPs on the internal and external of TiO_2 shell. The highly dispersed PNPs on TiO_2 support may enhance the catalytic activity and stability.[16] The EDX elemental mapping clearly displays that the @Pd/meso-TiO_2/Pd@meso-SiO_2 nanocatalyst is composed of inner TiO_2 and outer SiO_2 shells with PNPs uniformly distributed on the internal and external surfaces of TiO_2 shells (Fig. 1f). In particular, it can be confirmed from EDX elemental mapping image that a large quantity of PNPs with very small size (~5 nm) exist in the nanocatalyst, which may be advantageous for improving the catalytic performance.[26] The SEM images further indicate that the " shell-in-shell" structured @Pd/meso-TiO_2/Pd@meso-SiO_2 nanocatalyst has relatively smooth surface, better monodispersity, and good integrity (Figs. 1g, h, and S3).

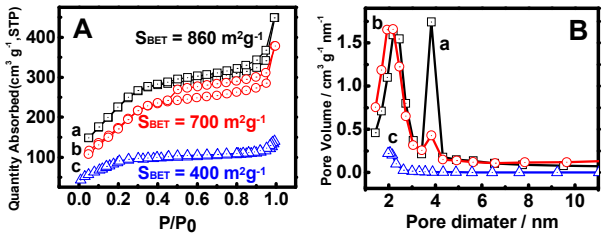

Fig. 2 Nitrogen adsorption-desorption isotherm (A) and BJH pore size distribution (B) of (a) @meso-TiO_2/Pd@meso-SiO_2, (b) @Pd/meso-TiO_2/Pd@meso-SiO_2, and (c) @meso-TiO_2/Pd^{2+}@RF@SiO_2 nanocatalysts.

The enlarged image of a crack sphere further demonstrates the double-shell structure of the @Pd/meso-TiO_2/Pd@meso-SiO_2 nanocatalyst. The XRD partern of the nanocatalyst displays a diffraction peak attributed to SiO_2 (Figs.1i and S5). The diffraction peaks of TiO_2 and PNPs are not detectable mainly because of the monnodispersity of PNPS with small size and the formation of amorphous TiO_2 shell. It may suggests that the RF and m-SiO_2 shell can pervent the heat from conducting to the inner shell during the calcination process, and effect on the crystallization of TiO_2 shell (Fig. S6). Such mesoporous "shell-in-shell" structured nanocatalyst may greatly improve its catalytic performance for various reactions.

Fig. 2 show the nitrogen adsorption–desorption isotherm and BJH pore size distribution of @Pd/meso-TiO_2/Pd@meso-SiO_2 nanocatalyst. It displays a typical IV isotherm with H1-type hysteresis loops (P/P_0 > 0.5), indicating the presence of mesopores in TiO_2 and SiO_2 shells. The nanocatalyst has a relatively high surface area (~700 $m^2 \cdot g^{-1}$). The BJH pore size distribution shows that the nanocatalyst has two obvious pore sizes (~2.2 and ~3.8 nm) attributed to the mesoporous SiO_2 and TiO_2 shells[12,27] in consistence with the SAXRD result (Fig. S7), which is beneficial for improving its catalytic activity.

In order to verify the superority of such featured nanocatalyst on catalysis, the Suzuki-Miyaura coupling and 4-nitrophenol reductions are employed as model reactions to evaluate the catalytic capability of the @Pd/meso-TiO_2/Pd@meso-SiO_2 nanocatalyst. As contrast, the @meso-TiO_2/Pd@meso-SiO_2 @meso-TiO_2/Pd@SiO_2, @Pd/meso-TiO_2/Pd, and @meso-TiO_2/Pd nanocatalysts were also synthesized according to the synthetic procedures illustrated in Scheme S1 (Fig. S8). Based on the catalytic performance of different nanocatalysts on Suzuki-Miyaura coupling reaction under varible base, solvent, and temperature conditions (Tables S1-4). The @Pd/meso-TiO_2/Pd@meso-SiO_2 displays the outstanding catalytic performance on Suzuki-Miyaura coupling reaction of halogeno benzene and phenylboronic acid (Table 1, Entries 1 and 2).[3,28] A 99% conversion of iodobenzene can be realized within 10 min, and the turnover frequency (TOF) can reach as high as 15390 h^{-1}, higher than most of previously reported heterogeneous catalysts.[16] It also exhibits high bromobenzene conversion with a onversion of 99% and a TOF of 3961 h^{-1} within 60 min.

For comparison, the catalytic performance of the contrast @meso-TiO_2/Pd@meso-SiO_2, @meso-TiO_2/Pd@SiO_2, @Pd/meso-TiO_2/Pd, and @meso-TiO_2/Pd nanocatalysts are also evaluated (Table S1). It can be clearly seen that the "shell in shell" structured @Pd/meso-TiO_2/Pd@meso-SiO_2 nanocatalyst

Table 1 Suzuki–Miyaura coupling reactions of aryl halides on @Pd/meso-TiO_2/Pd@meso-SiO_2 nanocatalyst[a]

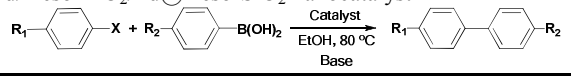

Entry	X	R_1	R_1	Base	T./min	Con./%[b]	TOF/h^{-1}[c]
1	I	-H	-H	Cs_2CO_3	10	99	15390
2	Br	-H	-H	Cs_2CO_3	60	99	3961
3	I	$-NO_3$	-H	Cs_2CO_3	10	100	15546
4	I	-F	-H	Cs_2CO_3	10	99	15390
5	I	-OH	-H	Cs_2CO_3	10	99	15390
6	I	-COOH	-H	Cs_2CO_3	10	97	15078
7	I	$-OCH_3$	-H	Cs_2CO_3	10	96	14925
8	I	$-CH_3$	-H	Cs_2CO_3	10	95	14769
9	I	$-NH_2$	-H	Cs_2CO_3	10	88	13680
10	I	$-COCH_3$	-H	Cs_2CO_3	10	53	8220
11	I	H	-nBu	Cs_2CO_3	10	90	13992
12	I	H	-tBu	Cs_2CO_3	10	trace	–

[a] Reaction conditions: 80 °C, ethanol (10 mL), iodobenzene or bromobenzene (0.5 mmol), phenylboronic acid (1 mmol), K_2CO_3 or Cs_2CO_3 (1 mmol), catalyst (10 mg or 25 mg), reaction time (10 min or 60min)

[b] Determined by HPLC using pentamethylbenzene as internal standard.

[c] TOF is defined as the moles of reacted aryl halides molecules per mole of Pd atom in catalyst per hour.

exhibits higher catalytic activity than @meso-TiO_2/Pd@meso-SiO_2, @meso-TiO_2/Pd@SiO_2, @Pd/meso-TiO_2/Pd, and @meso-TiO_2/Pd nanocatalysts.Combining with the Pd content in different catalysts, we deduce that the outstading catalytic performance of @Pd/meso-TiO_2/Pd@meso-SiO_2 nanocatalyst may be mainly ascribed to it unique structural configuration.[29] First, two independent chambers composed of double shells of TiO_2 and SiO_2 in the nanocatalyst can act as a nanoreactor to gather the reactants and further accelerate the catalytic reaction rate due to the confinement effect of microenvironments, which is proven by the absorption experiments (Fig. S9). Second, the "shell-in-shell" architecture also allows the Pd nanoparticles uniformly dispersed on the internal and external surfaces of TiO_2 shell, which may enrich the PNPs active sites and increase the contact area between reactants and catalysts to enhance the synergy between PNPs and TiO_2. In addition, the "shell-in-shell" @Pd/meso-SiO_2/Pd@meso-SiO_2 catalyst shows the less leaching of Pd in comparison with the traditional catalyst (Table S5). This suggests that the double-shell architecture of @Pd/meso-TiO_2/Pd@meso-SiO_2 catalyst may be effective for preventing the leaching of Pd from the internal and external surfaces of inner TiO_2 walls, which may be beneficial for the improvement of catalytic performance.[7] The XPS result shows that the PNPs in double-shell nanoreactor exists in the valence state of Pd^0 (Fig. S10), which may possess superior catalytic activity. Third, the –OH group on the surface of amorphous TiO_2 shell, as proven by FT-IR result (Fig. S11 and 12), is in favor of catalyzing Suzuki-Mayura coupling reaction.[30] Fourth, the mesoporous TiO_2 and SiO_2 shells facilitate the fast diffusion of reactants and products from the active sites on TiO_2 shell, which is beneficial for heterogeneous catalysis according to the tests shown in Table S6.[31] Last, the large specific surface area can increase the exposure of the active component in the nanocatalysts, thus promoting the catalytic performance. Thus, the double-shell architecture can be expected to be unique catalyst system for tuning the catalytic performance by manipulating its shell porosity, interstitial spaces, and configuration on micro- and nano-scales.[32] In addition, various aryl iodides with different substituents are used to investigate the reaction scopes of @Pd/meso-TiO_2/Pd@meso-SiO_2 nanocatalyst (Table 1, Entries 2-10). The results display that @Pd/meso-TiO_2/Pd@meso-SiO_2 nanocatalyst possesses outstanding catalytic performance for iodobenzene containing $-CH_3$, $-OCH_3$, $-NH_2$, $-NO_3$,-COOH, -F, $-COCH_3$ and -OH groups. The biaryl yields can reach 53-99 % within 10 min. Meanwhile, according to the catalytic results shown in Table 1 (Entries 11 and 12), we can infer that the mesopores in SiO_2 shell may be selectively make the reactants diffuse into the nanoreactor owing to the pore size and shape to achieve catalytic selectivity for different reactants depending on the reatant molecules.[21,22] Due to the unique "shell-in-shell" architecture configuration, the "shell-in-shell" @Pd/TiO_2/Pd@meso-SiO_2 nanocatalyst also show the super performance with high catlytic activity and stability for the reduction of 4-nitrophenol to 4-aminophenol (Fig. S13).

Conclusions

We presented a well-controlled strategy to construct novel a mesoporous "shell-in-shell" @Pd/meso-TiO_2/Pd@meso-SiO_2 nanocatalyst composed of mesoporous double TiO_2 and SiO_2 shells with PNPs uniformly distributed on the external and internal TiO_2 shell. The unique structural configureation endows the nanocatalyst unusual features of large specific surface area, mesoporous TiO_2 and SiO_2 shells, two independent nanoreactors, good dispersity and decreased leaching of PNPs, and enhanced synergistic effects. These features can largely improve the catalytic activity and stability of the nanocatalyst, leading to extremely high catalytic activity for Suzuki Miyaura coupling and 4-nitrophenol reduction reactions with TOFs of 15390 h^{-1} and 760 h^{-1}, respectively for the mesoporous "shell-in-shell" @Pd/meso-TiO_2/Pd@meso-SiO_2 nanocatalyst. The catalytic stability is also superior with the conversion remaining over 89% even after ten cycles of catalytic reaction for 4-nitrophenol reduction. The synthetic methodology may be provide a effective route to create highly efficient ananocatalysts. As the synthetic procedures involve multi-steps, the simplification of the synthetic process is under investigation and will be addressed elsewhere.

Acknowledgement

This work was supported by NSFC (21261011), NSFC (21201097),Program for New Century Excellent Talents in University (NCET-10-0907), Application Program from Inner Mongolia Science and Technology Department (2011401), Inner Mongolia "Grassland Talent" Program, and Natural Science Foundation of Inner Mongolia Autonomous Region of China (2014MS0506).

Notes and references

[a] *College of Chemistry and Chemical Engineering, Inner Mongolia University, Hohhot 010021, P. R. China. Fax: 0086 471 4992278; Tel: 0086 471 4992175; E-mail: cejzhang@imu.edu.cn*

[b] *College of Life Science, Inner Mongolia University, Hohhot 010021, P. R. China*

[c] *Inner Mongolia Key Lab of Nanoscience and Nanotechnology, Inner Mongolia University, Hohhot 010021, P. R. China*

† Electronic Supplementary Information (ESI) available: [detailed synthetic procedures, catalytic performance, SEM, TEM, EDX, XRD, FT-IR, and XPS]. See DOI: 10.1039/b000000x/

1. Y. Zhang, X. Cui, F. Shi and Y. Deng, *Chem. Rev.*, 2011, **112**, 2467-2505.
2. A. Balanta, C. Godard and C. Claver, *Chem. Soc. Rev*., 2011, **40**, 4973-4985.
3. H. Lorenz, C. Rameshan, T. Bielz, N. Memmel, W. Stadlmayr, L. Mayr, Q. Zhao, S. Soisuwan, B. Klotzer and S. Penner, Chemcatchem, 2013, **5**, 1273-1285.
4. M. Pérez-Lorenzo, B. Vaz, V. Salgueiriño and M. A. Correa-Duarte, *Chem -A. Eur. J*., 2013, **19**, 12196-12211.
5. B. Li, W. Z. Weng, Q. Zhang, Z. W. Wang and H. L. Wan, *ChemCatChem*, 2011, **3**, 1277-1280.
6. W. F. Yan, S. M. Mahurin, Z. W. Pan, S. H. Overbury and S. Dai, *J. Am. Chem. Soc*., 2005, **127**, 10480-10481.
7. J. L. Shi, Chem. Rev., 2013, **113**, 2139-2181.
8. X. Chen and S. S. Mao, *Chem. Rev.*, 2007, **107**, 2891-2959.
9. X. D. Wang, Z. D. Li, J. Shi and Y. H. Yu, *Chem. Rev*., DOI:10.1021/cr400633s.
10. L. Z Wang and T. Sasaki, *Chem. Rev.*, DOI: 10.1021/cr400627u.
11. Z. Jin, M. D. Xiao, Z. H. Bao, P. Wang and J. F. Wang, *Angew. Chem., Int. Ed*., 2012, **51**, 6406-6410.
12. J. B. Joo, Q. Zhang, M. Dahl, I. Lee, J. Goebl, F. Zaera and Y. D. Yin, *Energy Environ. Sci*, 2012, **5**, 6321-6327.
13. J. B. Joo, Q. Zhang, I. Lee, M. Dahl, F. Zaera and Y. D. Yin, *Adv. Funct. Mater*., 2012, **22**, 166-174.
14. Z. Y. Wang, Z. C. Wang, S. Madhavi and X. W. Lou, *Chem-A-Eur. J,* 2012, **18**, 7561-7567.
15. J. Du, J. Qi, D. Wang and Z. Y. Tang, *Energ. Environ. Sci*., 2012, **5**, 6914-6918.
16. Y. Yu, C. Y. Cao, Z. Chen, H. Liu, P. Li, Z. F. Dou and W. G. Song, *Chem. Comm*., 2013, **49**, 3116-3118.
17. B. Wang, C. Li, H. Cui, J. Zhang, J. P. Zhai and Q. Li, *Chem. Eng. J*., 2013, **223**, 592-603.
18. Y. Li and J. Shi, *Adv. Mater.* , 2014, **26**, 3176-3205.
19. J. Liu, S. Z. Qiao, J. S. Chen, X. W. Lou, X. Xing and G. Q. Lu, *Chem. Commun*., 2011, **47**, 12578-12591.
20. C. Q. Chen, J. Qu, C. Y. Cao, F. Niu and W. G. Song, *J. Mater. Chem*., 2011, **21**, 5774-5779.
21. J. Liu, H. Q. Yang, F. Kleitz, Z. G. Chen, T. Yang, E. Strounina, G. Q. M. Lu and S. Z. Qiao, *Adv. Funct. Mater.,* 2012, **22**, 591-599.
22. Z. Chen, Z.-M. Cui, P. Li, C.-Y. Cao, Y.-L. Hong, Z.-y. Wu and W.-G. Song, *J. Phys. Chem C*., 2012, **116**, 14986-14991.
23. J. Liu, S. Z. Qiao, H. Liu, J. Chen, A. Orpe, D. Zhao and G. Q. Lu, *Angew. Chem., Int. Ed*., 2011, **50**, 5947-5951.
24. X. Fang, J. Zang, X. Wang, M.-S. Zheng and N. Zheng, *J. Mater. Chem. A.*, 2014, **2**, 6191-6197
25. T. Yang, J. Liu, Y. Zheng, M. J. Monteiro and S. Z. Qiao, *Chem. Eur. -A. J.*, 2013, **19**, 6942-6945.
26. J. C. Park, E. Heo, A. Kim, M. Kim, K. H. Park and H. Song, *J. Phys. Chem C.*, 2011, **115**, 15772-15777.
27. Z. Chen, Z. M. Cui, F. Niu, L. Jiang and W. G. Song, *Chem. Comm*., 2010, **46**, 6524-6526.
28. A. Fihri, M. Bouhrara, B. Nekoueishahraki, J. M. Basset and V. Polshettiwar, *Chem. Soc. Rev*., 2011, **40**, 5181-5203.
29. B. Liu, S. Yu, Q. Wang, W. Hu, P. Jing, Y. Liu, W. Jia, Y. Liu, L. Liu and J. Zhang, *Chem. Comm*., 2013, 49, 3757-3759.
30. Z. Gao, Y. Feng, F. Cui, Z. Hua, J. Zhou, Y. Zhu and J. Shi, *J. Mol. Catal A: Chem.*, 2011, **336**, 51-57.
31. Z. Chen, Z.-M. Cui, F. Niu, L. Jiang and W.-G. Song, *Chem. Comm.*, 2010, **46**, 6524-6526.
32. X. Lai, J. E. Halpert and D. Wang, *Energy Environ. Sci*., **2012**, 5, 5604-5618.